Spt5 modulates co-transcriptional spliceosome assembly in Saccharomyces cerevisiae

Spt5 modulates co-transcriptional spliceosome assembly in *Saccharomyces cerevisiae*

Isabella E. Maudlin* and Jean D. Beggs

Wellcome Centre for Cell Biology, School of Biological Sciences, University of Edinburgh, King's Buildings, Edinburgh EH9 3BF, UK.

*Corresponding author

E-mail: bllmdln@gmail.com

Short title: Spt5 modulates co-transcriptional spliceosome assembly

Key words: transcription, pre-mRNA splicing, yeast

Abstract

There is increasing evidence from yeast to humans that pre-mRNA splicing occurs mainly co-transcriptionally, such that splicing and transcription are functionally coupled. Currently, there is little insight into the contribution of the core transcription elongation machinery to co-transcriptional spliceosome assembly and pre-mRNA splicing. Spt5 is a member of the core transcription elongation machinery and an essential protein, whose absence in budding yeast causes defects in pre-mRNA splicing. To determine how Spt5 affects pre-mRNA splicing, we used the auxin-inducible degron system to conditionally deplete Spt5 in *Saccharomyces cerevisiae* and assayed effects on co-transcriptional spliceosome assembly and splicing. We show that Spt5 is needed for efficient splicing and for the accumulation of U5 snRNPs at intron-containing genes, and therefore for stable co-transcriptional assembly of spliceosomes. The defect in co-transcriptional spliceosome assembly can explain the relatively mild splicing defect as being a consequence of the failure of co-transcriptional splicing. Co-immunoprecipitation of Spt5 with core spliceosomal proteins and all spliceosomal snRNAs suggests a model whereby Spt5 promotes co-transcriptional pre-mRNA splicing by stabilising the association of U5 snRNP with spliceosome complexes as they assemble on the nascent transcript. If this phenomenon is conserved in higher eukaryotes, it has potential to be important for co-transcriptional regulation of alternative splicing.

Introduction

Genes in most eukaryotes contain non-coding sequences ('introns') that interrupt the coding sequences ('exons'). Introns are present in the nascent transcripts (pre-mRNAs) and are excised and the exons joined in a process called pre-mRNA splicing. Introns are defined by short conserved sequences: the 5' splice site (5'SS), the 3'SS and the branch point (BP). *Trans*-acting factors recognise these motifs and position the pre-mRNA for the two transesterification reactions catalysed by the spliceosome. The spliceosome is a large macromolecular complex composed of small nuclear ribonucleoprotein particles (snRNPs) – U1, U2, U4/ U6 and U5 - and many non-snRNP proteins (reviewed in Hoskins and Moore, 2012). Both *in vitro* and *in vivo*, the snRNPs assemble on the pre-mRNA in a step-wise manner. First, the U1 snRNP binds to the 5'SS, and the U2 snRNP binds to the BP, forming the pre-spliceosome, or A complex. The U4/U6•U5 tri-snRNP then joins, forming the pre-catalytic spliceosome, or pre-B intermediate complex, which is unstable (Boesler et al. 2016). The pre-B complex undergoes substantial re-arrangements to produce the B complex in which the tri-snRNP is stably associated. The spliceosome undergoes further structural rearrangements to form the catalytically active B* complex, that catalyses the first step of splicing. Further rearrangements promote the second catalytic step that generates the spliced RNA and then the spliceosome dissociates. The splicing factors are then recycled for a new round of splicing (reviewed in Will and Lührmann, 2011).

There is increasing evidence from lower to higher eukaryotic organisms that splicing occurs mainly co-transcriptionally - that is, spliceosomes assemble and splicing catalysis occurs as RNA polymerase II (RNAPII) transcribes along the gene, before transcription termination (Kotovic et al. 2003; Görnemann et al. 2005; Lacadie and Rosbash, 2005; Listerman et al.

2006; Carillo Oesterreich et al. 2010; Ameur et al. 2011; Khodor et al. 2011; Tilgner et al. 2012; Brugiolo et al. 2013; Nojima et al. 2015; Carillo Oesterreich et al. 2016; Harlen et al. 2016; Wallace and Beggs, 2017). By definition, co-transcriptional splicing occurs in close proximity to the transcription elongation machinery and it is well-established that transcription and splicing are functionally coupled such that they influence one another (Fong and Zhou 2001; de la Mata et al. 2003; Howe et al. 2003; Alexander et al. 2010a; Ip et al. 2011; Braberg et al., 2013; Chathoth et al. 2014; Dujardin et al. 2014; Fong et al. 2014; Aslanzadeh et al. 2018). There are two non-mutually-exclusive models for how transcription affects splicing: (i) the speed of RNAPII elongation affects intron/exon recognition (termed the 'kinetic' model) and/or (ii) the transcription elongation machinery facilitates recruitment of splicing factors to the site of transcription (termed the 'recruitment' model) (reviewed in Kornbihtt et al. 2004; Bentley 2005; de la Mata et al. 2005; Perales and Bentley, 2009; Bentley, 2014; Dujardin et al. 2013; Merkhofer et al. 2014).

Spt5 is the most highly conserved core transcription elongation factor that, following initiation of transcription, associates tightly with RNAPII during elongation until transcription termination, and acts as a docking site for protein complexes that influence RNAPII processivity, RNA processing and histone modifications (reviewed in Hartzog and Fu, 2013). It is thought that Spt5 enhances RNAPII processivity by stabilising interaction between its clamp domain and the DNA template (Hirtreiter et al. 2010; Klein et al. 2011; Martinez-Rucobo et al. 2011). In metazoans, DSIF (Spt4/5 in *S. cerevisiae*) and NELF cause RNAPII to pause in a stable manner downstream of transcription start sites, referred to as promoter-proximal pausing (reviewed in Adelman and Lis, 2012). Depletion of Spt5 in *Schizosaccharomyces pombe* causes genome-wide defects in transcription elongation (Shetty et al. 2017). In mammals, Spt5 depletion does not cause such genome-wide defects but seems

to be important for elongation only on long genes (Fitz et al. 2018). Spt5 has a conserved but non-essential C-terminal region (CTR) that is differentially phosphorylated during the course of transcription, and is important for RNAPII elongation and histone modification (Zhou et al., 2009). In particular, phosphorylation of the CTR of Spt5 by the Bur1/2 kinase complex is important for Paf1 complex (Paf1C) recruitment to elongating RNAPII (Laribee et al. 2005; Liu et al. 2009). Paf1C is associated with RNAPII along actively transcribed genes where it serves as a 'platform' that co-ordinates the association of transcription factors and chromatin-modifying enzymes with RNAPII, thereby facilitating transcription elongation (reviewed in Jaehning, 2010). Paf1C is required for H2BK123 mono-ubiquitination, which in turn is required for H3K4 di- and tri-methylation (Wood et al. 2003; Krogan et al. 2003; Ng et al. 2003; Xiao et al. 2005b). The Paf1 complex also affects H3K36 tri-methylation (Chu et al. 2007).

There is evidence that Spt5 affects the pre-mRNA splicing outcome. For example, mutations in Spt5 or its partner, Spt4, result in splicing defects in *S. cerevisiae* (Lindstrom et al. 2003; Burckin et al. 2005; Xiao et al. 2005a), and depletion of Spt4 in mammalian cells results in changes to alternative splicing patterns (Liu et al. 2012). Further, depletion of Spt5 in mammalian cells causes pre-mRNA accumulation on some genes (Diamant et al. 2012). Similarly, depletion of Spt5 in *S. pombe* causes pre-mRNA accumulation, as shown by RNA sequencing (Shetty et al. 2017). Additionally, it was shown in yeast that Spt5 is enriched on intron-containing genes compared to intronless genes (known as "intron bias") and that Spt5 co-immunoprecipitates with Prp40, a core protein of the U1 snRNP (Moore et al. 2006). Further, Spt5 was found to crosslink more to pre-mRNA intron sequences compared to exon sequences in *S. cerevisiae* (Battaglia et al. 2017).

Collectively, these studies demonstrate that Spt5 is important for splicing outcome, but there is no clear insight into how this happens. As Spt5 functions during transcription, it seems likely that it affects splicing co-transcriptionally although, apparently, this has not been investigated. Here, an auxin-inducible degron (AID) system (Nishimura et al. 2009; Mendoza-Ochoa et al. 2018) was used to conditionally deplete Spt5 in *S. cerevisiae*, and effects on co-transcriptional spliceosome assembly and splicing were investigated. Analysis of co-transcriptional spliceosome assembly showed that depletion of Spt5 did not affect co-transcriptional U1 or U2 snRNP recruitment, meaning at least the pre-spliceosome or A complex can form co-transcriptionally in the absence of Spt5. However, co-transcriptional recruitment of the U5 snRNP was reduced, indicating that B complex cannot efficiently or stably form co-transcriptionally in the absence of Spt5. Further, Spt5 pulls down all spliceosomal snRNAs and co-immunoprecipitates with spliceosomal proteins. We propose that Spt5 affects U5 snRNP recruitment and pre-B and/or B complex formation co-transcriptionally through interaction with components of the spliceosome. Together, these data provide insight into how Spt5 could specifically affect co-transcriptional pre-mRNA splicing to cause a mild splicing defect in *S. cerevisiae*.

Results

Use of the AID system to conditionally deplete Spt5

To determine whether the physical presence of Spt5 affects co-transcriptional spliceosome assembly *in vivo* in *S. cerevisiae*, Spt5 was conditionally depleted using the AID system. Spt5 was C-terminally tagged with the AID* degron and 6xFLAG epitope in a strain that allowed conditional induction with β-estradiol of OsTIR1, the auxin-binding receptor protein from *Oryza sativa* (McIsaac et al. 2013; Mendoza-Ochoa et al. 2018). Following addition of β-estradiol and auxin to the culture, the auxin-bound OsTIR1 targets the Spt5-AID* protein for ubiquitylation and degradation by the proteasome. Western blotting showed that treatment for 40 minutes resulted in the reduction of Spt5-AID* to 40%, on average, of the undepleted amount (Figure 1A). Chromatin immunoprecipitation and quantitative PCR (ChIP-qPCR) analysis across three intron-containing genes (Figure 1B) showed that, in wild-type conditions, Spt5-AID* occupancy peaks over introns and exon 2 of the genes analysed (Figure 1C). After auxin treatment, Spt5-AID* was significantly depleted at each of the intron-containing genes tested (Figure 1C).

Depletion of Spt5 reduces the co-transcriptional recruitment of the U5 snRNP without affecting co-transcriptional pre-spliceosome assembly

As splicing factors assemble co-transcriptionally, their close proximity to chromatin enables them to be crosslinked to the DNA template and analysed by ChIP-qPCR. In this way, the co-transcriptional recruitment of splicing factors and spliceosome assembly can be monitored *in vivo* (Kotovic et al. 2003; Görnemann et al. 2005; Lacadie and Rosbash, 2005; Tardiff and

Rosbash, 2006). ChIP was performed, using antibodies against core members of the spliceosome, to determine whether depletion of Spt5 affects co-transcriptional spliceosome assembly at the intron-containing genes *ACT1*, *RPS13* and *ECM33*. These three genes are well expressed and their transcripts are co-transcriptionally spliced (Wallace and Beggs, 2017). Antibodies were used that detect Prp40 (U1 snRNP), Lea1-3HA (U2 snRNP) or Prp8 (U5 snRNP), which allowed a determination of which stage, if any, of co-transcriptional spliceosome assembly may be affected by depletion of Spt5. In conditions without auxin or β-estradiol, the ChIP profiles of U1 snRNP (Prp40), U2 snRNP (Lea1-3HA) and U5 snRNP (Prp8), were as expected; the U1 and U2 snRNP signals peaked near the 3'SS, and the U5 snRNP peaked nearer the 3'end of the gene. ChIP-qPCR showed that depletion of Spt5 for 40 minutes did not significantly or consistently affect U1 or U2 snRNP occupancies on the intron-containing genes tested (Figure 2A and 2B), relative to conditions without depletion. In contrast, depletion of Spt5 resulted in a significant reduction in U5 snRNP occupancy where it normally peaks on *ACT1* (amplicon 5, exon 2), on *RPS13* (amplicon 5, exon 2) and on *ECM33* (amplicons 4 and 5, exon 2) (Figure 2C). Moreover the U5 ChIP signal declined prematurely compared with normal.

It is conceivable that reduced U5 snRNP recruitment could be an indirect consequence of reduced RNAPII occupancy following Spt5 depletion, for example, causing loss of interactions between certain splicing factors and RNAPII. However, ChIP using an antibody against RNAPII (Rpb1) (Figure 2D) showed no consistent effect on RNAPII occupancy across these intron-containing genes. Moreover, western blotting, performed with extracts from cells grown with or without 40 minutes of auxin treatment, showed no significant difference in the total cellular level of Prp8 protein upon Spt5 depletion (Figure 2E), indicating that the observed loss of U5 snRNP occupancy, as measured by ChIP of Prp8 following Spt5 depletion, was not simply due to a reduction in the total cellular level of the Prp8 protein.

188 **Depletion of Spt5 causes defects in pre-mRNA splicing**

189

190 Next, the effect of Spt5 depletion on splicing was investigated for the same intron-containing
191 genes (*ACT1*, *RPS13* and *ECM33*). In order to distinguish defects at different stages of splicing
192 catalysis, reverse transcriptase real-time quantitative PCR (RT-qPCR) assays were performed
193 using primers that distinguish unspliced pre-mRNA, lariat (excised intron lariat or lariat-exon
194 2) and spliced exons (Figure 3A). An increase in 3'SS and 5'SS or BP signals is indicative of
195 pre-mRNA accumulation and a first step splicing defect. Increased signals for 3'SS and lariat
196 is indicative of a second step splicing defect (lariat-exon 2). Increased lariat signal only
197 (without 3'SS or BP accumulation) suggests accumulation of the excised intron-lariat. RT-
198 PCR of lariat species involves using a primer that spans the conserved branchsite of the lariat.
199 Of the genes tested, only *ACT1* lariats can be reliably measured this way.

200

201 RT-qPCR on total (steady state) RNA showed that depletion of Spt5 resulted in accumulation
202 of pre-mRNA for *ACT1* (BP and 3'SS signals) *ECM33* (5'SS signal) and *RPS13* (5'SS signal),
203 indicating a first step defect in pre-mRNA splicing (Figure 3B, Supplementary Figure S1). In
204 the case of *ACT1* we were also able to quantify lariat species, which shows that depletion of
205 Spt5 resulted in a reduction in lariat signal, supporting a first step splicing defect (Figure 3B,
206 Supplementary Figure S1). The observation that the levels of the spliced mRNAs were not
207 significantly changed likely reflects the relatively short Spt5 depletion time as well as the
208 relatively mild splicing defect.

209

210 **Spt5 interacts with snRNPs**

211

RNA immunoprecipitation (RIP) was performed in which Spt5-AID*-6FLAG was pulled down using a FLAG antibody and associated RNA was purified followed by RT-qPCR to detect any association of Spt5 with U1, U2, U4, U5 and U6 spliceosomal RNAs. RIP analysis showed Spt5 interacting mostly with the U1 snRNA, and also with U2, U4, U5 and U6 snRNAs significantly above background (Figure 4A). RT-qPCR of intron-containing transcripts showed Spt5 pulling down more pre-mRNAs in comparison with spliced RNAs, in agreement with previous studies, which found that Spt5 exhibited intron bias and interaction with nascent pre-mRNAs (especially introns) (Figure 4B) (Moore et al. 2006; Battaglia et al. 2017). To investigate the possibility of an interaction between Spt5 and spliceosomal proteins, co-immunoprecipitation experiments were performed in which Spt5-AID*-6FLAG was pulled down using a FLAG antibody, followed by western blotting with antibodies against Prp40 (U1), Lea1-3HA (U2) and Prp8 (U5). As shown in Figure 4C, Prp8 was specifically co-immunoprecipitated with Spt5-AID*-6FLAG and, as the addition of RNase did not affect the co-immunoprecipitation, this interaction appears to be RNA-independent. No pull down of Prp8 was detected using a control strain with untagged Spt5, confirming the specificity of the co-immunoprecipitation. Although Prp40 (U1 snRNP) and Lea1 were not detected in the pull down of Spt5 (Figure 4C), immunoprecipitation of Prp40, Lea1 and Prp8 each co-immunoprecipitated Spt5 in an RNase-resistant manner (Figure 4D). Therefore, Spt5 appears to interact with several core spliceosomal proteins, but only the co-immunoprecipitation between Spt5-AID*-6FLAG and Prp8 was reciprocal. RT-qPCR analysis demonstrated the effectiveness of the RNase treatment for both snRNAs and pre-mRNA (Figure 4E).

The effect of Spt5 depletion on co-transcriptional recruitment of the U5 snRNP is not Paf1-dependent

To test whether the effect of Spt5 depletion on co-transcriptional spliceosome assembly was due to loss of Paf1C, a core member of the complex, Paf1, was depleted by the AID system and effects on co-transcriptional spliceosome assembly were determined. Western blotting showed that 30 minutes of auxin treatment resulted in a significant reduction in Paf1-AID* to, on average, 8% relative to cells without auxin treatment (Figure 5A). ChIP-qPCR analysis showed that, in addition to being depleted in whole cell extracts, Paf1 was significantly depleted across the intron-containing genes tested after auxin treatment (Figure 5B). However, in contrast to the effect of depleting Spt5, ChIP-qPCR analysis showed no significant change in the occupancy of the U5 snRNP at *ACT1, ECM33* or *RPS13*, following 30 minutes of Paf1-AID* depletion, relative to conditions prior to auxin addition (Figure 5C, Supplementary Figure S2). Nor were consistent changes in U1 or U2 snRNP occupancy observed (data not shown).

To determine whether Paf1-AID* depletion affected pre-mRNA splicing, RT-qPCR was performed, as described above, on total (steady-state) RNA. No significant change in the levels of the pre-mRNA, spliced exons or exon 2 was observed for *ACT1*, *RPS13* and *ECM33* following depletion of Paf1-AID*, relative to conditions prior to auxin addition (Figure 5D).

Discussion

There is some evidence that core members of the transcription elongation complex interact with splicing factors (Brés et al. 2005; Moore et al. 2006; Cao et al. 2015; Li et al. 2016), and can affect splicing outcome (Lindstrom et al. 2003; Burckin et al. 2005; Xiao et al. 2005a; Liu et al. 2012; Diamant et al. 2012; Shetty et al. 2017). However, there is currently little insight into how the core transcription elongation machinery affects co-transcriptional splicing or whether observed effects are direct or indirect (reviewed in Neugebauer, 2002; Merkhofer et al. 2014). Here, using the AID system to conditionally deplete transcription elongation factor Spt5, we provide insight into the contribution of Spt5 to pre-mRNA splicing in *S. cerevisiae.*

ChIP-qPCR, using antibodies against individual snRNP components, is a well-established method to monitor step-wise co-transcriptional spliceosome assembly (Kotovic et al. 2003; Görnemann et al. 2005; Lacadie and Rosbash, 2005; Tardiff and Rosbash, 2006). In particular, Prp8 is a reliable indicator of the presence of the U5 snRNP, as absence of Prp8 results in failure to form stable U5 snRNP or U4/U6.U5 tri-snRNP or their failure to assemble into spliceosomes (Brown and Beggs, 1992). It was also shown previously that pre-spliceosomes can form *in vivo* in the absence of the U5 snRNP (Tardiff and Rosbash, 2006). Following Spt5 depletion, we observed normal co-transcriptional recruitment of the U1 and U2 snRNPs but not of U5 snRNP to intron-containing genes (Figure 2), indicating unperturbed co-transcriptional assembly of the pre-spliceosome (A complex) but possible failure to form pre-B complex. However, the observation of a low level signal for U5 snRNP may indicate that transient pre-B complex forms but, in the absence of Spt5, dissociates, without convertion to B complex (Figure 2C) (Figure 6). Single molecule imaging analyses of spliceosome assembly *in vitro* have shown that individual stages of step-wise spliceosome assembly, including tri-snRNP association with the pre-spliceosome, are reversible in *S. cerevisiae* (Hoskins et al.

2011), and there is separate evidence that both steps of splicing can be reversed *in vitro* (Tseng and Cheng, 2008). Therefore, we cannot rule out the possibility that stable B complex forms and is rapidly converted to activated spliceosome that is itself unstable and is rapidly disassembled.

Although Spt5 promotes transcription elongation, the effects of Spt5 depletion on U5 snRNP recruitment are not simply due to altered transcription. Under the Spt5 depletion conditions used, the transcript levels did not significantly change (exon 2 in Figure 3B), nor did RNAPII occupancy (Figure 2D) change for the intron-containing genes tested. Moreover, changes to transcription would be predicted to affect the co-transcriptional recruitment of U1, U2 and U5 snRNPs similarly, whereas U1 and U2 snRNP recruitment was not changed by Spt5 depletion.

A defect in the co-transcriptional formation of spliceosomes can explain the observed mild splicing defect (Figure 3). This is consistent with previous studies in which mutations in Spt5 caused splicing defects in *S. cerevisiae*, and where depletion of Spt5 resulted in pre-mRNA accumulation in *S. pombe* (Lindstrom et al. 2003; Burckin et al. 2005; Shetty et al. 2017). It has been demonstrated that splicing is more efficient when co-transcriptional (Aslanzadeh et al. 2018), so that, although Spt5 likely does not affect post-transcriptional splicing, this does not compensate for lack of co-transcriptional splicing, explaining the relatively modest splicing defect observed when Spt5 was depleted.

How might this effect of Spt5 on co-transcriptional spliceosome assembly be mediated? Co-immunoprecipitation experiments showed a reciprocal association of Spt5 and Prp8 (Figures 4C and 4D). We also observed Prp40 (U1 snRNP) pull down of Spt5, which is in agreement with a previous study (Moore et al. 2006). However, Prp40 (U1) and Lea1 (U2) co-

304 immunoprecipitated Spt5 in a non-reciprical manner, which might suggest that these
305 interactions occur in the context of the spliceosome. Indeed, RIP experiments showed that Spt5
306 interacted with all 5 spliceosomal snRNAs (Figure 4A), with U1 snRNA being pulled down
307 the most, and that the intronic regions of the pre-mRNAs were enriched in the pull downs
308 compared with the exons (Figure 4B). Although the interactions of Spt5 with the snRNP
309 proteins are reproducibly all resistant to RNase treatment (Figures 4C and 4D), the intronic
310 regions of *ACT1* (the only transcript analysed by RT-qPCR after RNase treatment) were
311 relatively protected against the RNase treatment compared with the mRNA splice junction and
312 the snRNAs, therefore it cannot be ruled out that the Spt5 interactions with splicing factors are
313 intron-mediated. While our data are consistent with direct interactions between Spt5 and
314 splicing factors occurring *in vivo*, we cannot exclude the possibility that interactions may be
315 indirect or form post-lysis (Mili and Steitz, 2004). Assuming that these interactions occur *in*
316 *vivo*, as Spt5 is a transcription elongation factor, they presumably occur at sites of transcription
317 elongation.
318
319 The N-terminal region of Prp8 (U5 snRNP) has been reported to interact with several U1
320 snRNP proteins, including Prp40 (reviewed in Grainger and Beggs, 2005). Interestingly, the
321 conserved WW domains of Prp40 were proposed to bind the N-terminal part of Prp8p in yeast,
322 through proline-rich motifs (Abovich and Rosbash 1997; Wiesner et al. 2002), possibly
323 bridging interactions across the intron. In a functional analysis of the role of the Prp40 WW
324 domains in splicing, Görnemann et al. (2011) found that deletion of the Prp40 WW domains
325 reduced co-transcriptional U5 snRNP recruitment without affecting U1 or U2 snRNP
326 recruitment, similar to our findings for Spt5 depletion. It is therefore tempting to speculate that
327 Spt5 may promote interaction between Prp8, in the U5 snRNP, and Prp40 (and potentially other

U1 snRNP proteins) during tri-snRNP recruitment, thereby facilitating stable B complex formation co-transcriptionally, as indicated in our proposed model (Figure 6).

Together, these data provide insight into how Spt5 could affect pre-mRNA splicing, by modulating co-transcriptional recruitment or stable association of the U5 snRNP and/or tri-snRNP during spliceosome assembly, most likely by direct or indirect interaction with the spliceosome (Figure 6). We further show that the defect caused by Spt5 depletion is apparently not a consequence of failure to recruit the Paf1 complex to RNAPII (Figure 5), more directly implicating Spt5 itself, rather than recruitment of downstream transcription factors.

These results provide evidence of a role for a transcription elongation factor in co-transcriptional spliceosome assembly and thereby for the recruitment model of co-transcriptional splicing. As Spt5 is highly conserved, it will be of interest to determine whether Spt5 plays a similar role in co-transcriptional spliceosome assembly in higher eukaryotes, which is crucial for co-transcriptional regulation of alternative splicing.

Materials and Methods

Yeast strains and growth conditions

Yeast strains are listed in Table 1. Spt5 was C-terminally AID*-6FLAG tagged in a W303 strain containing a centromeric plasmid that allowed conditional induction of OsTIR1 using the β-estradiol system (McIsaac et al. 2013; Mendoza-Ochoa et al. 2018). Paf1 was C-terminally AID*-6FLAG tagged in the YBRT background strain. For tagging, a plasmid was used with the AID* cassette comprised of the AUX/IAA (AID*) recognition motif for auxin-mediated depletion and a 6 X FLAG tag for immunodetection (Morawska and Ulrich, 2013).

Auxin time course experiments

To induce TIR1 using the β-estradiol system, cells, grown in leucine-deficient yeast minimal media (YMM) to OD_{600} 0.7, were treated with 10 μM β-estradiol (Sigma-Aldrich #E8875; dissolved in 100% ethanol) to induce TIR1 expression and 0.75 mM Indole-3-acetic acid (IAA; auxin) (Acros organics #122160100) to deplete Spt5-AID*, for 40 minutes. To deplete Paf1-AID*, cells grown in YPDA medium to OD_{600} 0.7, were treated with 0.75 mM IAA for 30 minutes. After incubation with auxin, samples were taken for protein, RNA and chromatin extraction as described below.

Protein sample preparation and western blotting

Protein samples were prepared using a NaOH lysis and trichloroacetic acid (TCA) precipitation protocol (Volland et al. 1994). For western blotting, 25 μg of protein were run on a NuPAGE 4-12% Bis-Tris gel (Invitrogen #NP0323BOX) at 180 V in 1 X MOPS-SDS buffer (Invitrogen #1862491). Proteins were transferred to a Bio-rad nitrocellulose membrane (0.2 μm, #LC2009) using a semi-wet transfer unit (Bio-rad) at 100 V for 1 hour at 4℃ in Tris-Glycine transfer

buffer (200 mM Tris, 1.5 M glycine) with 10% methanol. After transfer, proteins of interest were visualised using the Odyssey infrared imaging system (LI-COR Bioscience), and quantified by the median method of the Odyssey software. Data were normalised against the 3-Phosphoglycerate Kinase (Pgk1) loading control. Primary and secondary antibodies used are listed in Table 2.

RNA preparation and RT-qPCR

RNA was extracted using a modified GTC:phenol method and RT-qPCR was performed as described in (Alexander et al. 2010b). A list of primers used for RT-qPCR can be provided upon request.

Chromatin immunoprecipitation (ChIP)

50 ml of culture at OD_{600} 0.8 was cross-linked in 1% (w/v) formaldehyde for 10 minutes with shaking at room temperature. The reaction was stopped by incubating the cells for 5 minutes with 2.5 ml of 2.5 M glycine. Cells were harvested by centrifugation and washed twice in ice-cold 1 X PBS. Cell pellets were re-suspended in 350 µl FA1 buffer (50 mM HEPES-KOH pH 7.5, 140 mM NaCl, 1mM EDTA pH 8.0, 1% Triton X-100, 0.1% sodium deoxycholate, one complete EDTA-free proteinase inhibitor tablet (Roche #11836145001), PhosSTOP tablets (Sigma Aldrich #000000004906845001)) and 350 µl zirconia beads. The cells were disrupted using the Mini-Beadbeater-24 (BioSpec Products) twice at 2000 rpm for 2 minutes with 2 minutes on ice in between. The sample was separated from the beads by centrifugation at 1000 x *g* for 2 minutes. The sample was centrifuged at 20,000 x *g* for 15 minutes at 4°C. The pellet was re-suspended in 600 µl FA1 buffer, and the sample sonicated using a New Twin Biorupt sonicator (Diagenode) for 15 cycles 30 seconds on and 30 seconds off. The sample was centrifuged at 20,000 x *g* for 30 minutes at 4°C and the supernatant containing solubilised

chromatin was retained. For immunoprecipitation, the appropriate amount of chromatin was incubated in 20 µl Protein A/G Dynabeads (Life Technologies #10001D/10003D) conjugated to antibody on a rotating wheel overnight at 4°C. A list of the antibodies for ChIP can be found in Table 2.

The beads were washed 3 times in FA1 buffer, twice in FA2 buffer (50 mM HEPES- KOH pH 7.5, 0.5 M NaCl, 1mM EDTA pH 8.0, 1% Triton X-100, 0.1% sodium deoxycholate), twice in FA3 buffer (10 mM Tris-HCl pH 8.0, 250 mM LiCl, 1mM EDTA pH 8.0, 0.5% NP-40, 0.5% Na deoxycholate) and once in Tris-EDTA pH 8.0 0.05% TWEEN-20. Crosslinking was reversed with 150 µl elution buffer (50 mM Tris- Hcl, 10 mM EDTA, 1% SDS) and 3 µl Proteinase K (25 mg/ml) and incubated at 42°C for 2 hours and 65°C overnight, shaking. An input sample equal to 10% of the protein that was used for the immunoprecipitation was prepared and crosslinking was reversed as above. The QIAGEN mini column clean-up kit was used to purify DNA according to the manufacturer's instructions, and DNA eluted in 400 µl of 10 mM Tris pH 8.0. Samples were analysed by qPCR as described above using primers that can be provided upon request. The ChIP data were normalised using the relative threshold cycle (Ct) values for each sample. ChIP data are presented as percentage of input normalised to the first amplicon of each gene.

Co-immunoprecipitation

250 ml of culture at OD_{600} 0.8 was harvested by centrifugation and washed twice in ice-cold 1 X PBS. The cell pellet was re-suspended in 900 µl lysis buffer (50 mM Tris-HCl pH 7.5, 2 mM Mg_2Cl_2, 150 mM NaCl, 0.2% NP-40, one complete EDTA-free proteinase inhibitor tablet (Roche #11836145001)) and 400 µl zirconia beads. Cells were lysed using a Mini-Beadbeater-24 as described above. The sample was centrifuged at 1000 x *g* for 2 minutes, the supernatant collected and further centrifuged at 20,000 x *g* for 30 minutes at 4°C and used for

immunoprecipitation. 50 µl Protein A/G Dynabeads (Life Technologies #10001D/10003D) conjugated to antibody were incubated with 1 mg of protein on a rotating wheel for 1 hour at room temperature. The beads were washed 8 times in lysis buffer. 20 µl of loading buffer was added to the beads, input and non-bound samples, which were boiled for 10 minutes before loading on a 4-12% Bis-Tris gel followed by western blotting as described above. A list of antibodies used for co-immunoprecipitation and subsequent western blotting can be found in Table 2.

For RNase treatment, 1 mg of protein was incubated with 100 µg/ml RNase A (Sigma Aldrich #R4642) for 30 minutes at room temperature prior to immunoprecipitation. The efficiency of RNase treatment was verified by RNA extraction and RT-qPCR as described above.

RNA immunoprecipitation

RNA immunoprecipitation was performed using a protocol modified from Churchman and Weissman, 2012. Cells at OD_{600} 0.8 were harvested by centrifugation and subjected to cryogeniclysis and DNase treatment as described in Churchmann and Weissman, 2012. For immunoprecipitation, 1 mg of lysate was incubated with 20 µl of dynabeads Protein A/G Dynabeads (Life Technologies #10001D/10003D) conjugated to antibody on a rotating wheel for 2 hours at 4°C. As a negative control, a mock pulldown using IgG was performed. The FLAG antibody used for immunoprecipitation can be found in Table 2. The beads were washed four times in lysis buffer. RNA was extracted and purified from input and pulldown samples using the Qiagen miRNeasy mini kit according to manufacturer's instructions. RIP data are presented as percentage of input. A list of primers used for RT-qPCR to detect snRNAs can be provided upon request.

Author contributions

IEM performed all experiments, JDB supervised the work, IEM and JDB jointly conceived of the project and wrote the manuscript.

Acknowledgements

This work was supported by Wellcome funding to JDB [104648] and a Wellcome Trust PhD studentship to IEM [105256]. Work in the Wellcome Centre for Cell Biology is supported by Wellcome core funding [092076].

References

Abovich N & Rosbash M (1997) Cross-intron bridging interactions in the yeast commitment complex are conserved in mammals. *Cell* **89:** 403–412

Adelman K & Lis JT (2012) Promoter-proximal pausing of RNA polymerase II: emerging roles in metazoans. *Nat. Rev. Genet.* **13:** 720–731

Alexander RD, Innocente SA, Barrass JD & Beggs JD (2010a) Splicing-Dependent RNA polymerase pausing in yeast. *Mol. Cell* **40**: 582–593

Alexander RD, Barrass JD, Dichtl B, Kos M, Obtulowicz T, Robert MC, Koper M, Karkusiewicz I, Mariconti L, Tollervey D, Dichtl B, Kufel J, Bertrand E & Beggs JD (2010b) RiboSys, a high-resolution, quantitative approach to measure the in vivo kinetics of pre-mRNA splicing and 3′-end processing in Saccharomyces cerevisiae. *RNA* **16:** 2570–2580

Ameur A, Zaghlool A, Halvardson J, Wetterbom A, Gyllensten U, Cavelier L & Feuk L (2011) Total RNA sequencing reveals nascent transcription and widespread co-transcriptional splicing in the human brain. *Nat. Struct. Mol. Biol.* **18:** 1435–1440

Aslanzadeh V, Huang Y, Sanguinetti G & Beggs JD (2018) Transcription rate strongly affects splicing fidelity and cotranscriptionality in budding yeast. *Genome Res.* **28:** 203–213

Battaglia S, Lidschreiber M, Baejen C, Torkler P, Vos SM & Cramer P (2017) RNA-dependent chromatin association of transcription elongation factors and pol II CTD kinases. *Elife* **6:** e25637

Bentley DL (2014) Coupling mRNA processing with transcription in time and space. *Nat. Rev. Genet.* **15:** 163–175

Bentley DL (2005) Rules of engagement: Co-transcriptional recruitment of pre-mRNA processing factors. *Curr. Opin. Cell Biol.* **17:** 251–256

Boesler C, Rigo N, Anokhina MM, Tauchert MJ, Agafonov DE, Kastner B, Urlaub H, Ficner R, Will CL & Lührmann R (2016) A spliceosome intermediate with loosely associated tri-snRNP accumulates in the absence of Prp28 ATPase activity. *Nat. Commun.* **7:** 11997

Braberg H, Jin H, Moehle EA, Chan YA, Wang S, Shales M, Benschop JJ, Morris JH, Qiu C, Hu F, Tang LK, Fraser JS, Holstege FCP, Hieter P, Guthrie C, Kaplan CD & Krogan NJ (2013) From structure to systems: High-resolution, quantitative genetic analysis of RNA polymerase II. *Cell* **154**: 775–788

Bres V, Gomes N, Pickle L & Jones KA (2005) A human splicing factor, SKIP, associates with P-TEFb and enhances transcription elongation by HIV-1 Tat. *Genes Dev.* **19:** 1211–1226

Brown JD & Beggs JD (1992) Roles of PRP8 protein in the assembly of splicing complexes. *EMBO J.* **11:** 3721–3729

Brugiolo M, Herzel L & Neugebauer KM (2013) Counting on co-transcriptional splicing. *F1000Prime Rep.* **5:** 5–9

Burckin T, Nagel R, Mandel-Gutfreund Y, Shiue L, Clark TA, Chong JL, Chang TH, Squazzo S, Hartzog G & Ares M (2005) Exploring functional relationships between components of the gene expression machinery. *Nat. Struct. Mol. Biol.* **12:** 175–182

Cao Y, Wen L, Wang Z & Ma L (2015) SKIP Interacts with the Paf1 Complex to Regulate Flowering via the Activation of FLC Transcription in Arabidopsis. *Mol. Plant* **8:** 1816–1819

Carrillo Oesterreich F, Herzel L, Straube K, Hujer K, Howard J & Neugebauer KM (2016) Splicing of Nascent RNA Coincides with Intron Exit from RNA Polymerase II. *Cell* **165:** 372–381

Carrillo Oesterreich F, Preibisch S & Neugebauer KM (2010) Global analysis of nascent rna reveals transcriptional pausing in terminal exons. *Mol. Cell* **40:** 571–581

Chathoth KT, Barrass JD, Webb S & Beggs JD (2014) A Splicing-Dependent Transcriptional Checkpoint Associated with Prespliceosome Formation. *Mol. Cell* **53**: 779–790

Chu Y, Simic R, Warner MH, Arndt KM & Prelich G (2007) Regulation of histone modification and cryptic transcription by the Bur1 and Paf1 complexes. *EMBO J.* **26:** 4646–4656

Churchman LS & Weissman JS (2012) Native elongating transcript sequencing (NET-seq). *Curr. Protoc. Mol. Biol.* **1:** 1–17

De La Mata M, Alonso CR, Kadener S, Fededa JP, Blaustein M, Pelisch F, Cramer P, Bentley D & Kornblihtt AR (2003) A slow RNA polymerase II affects alternative splicing in vivo. *Mol. Cell* **12**: 525–532

de la Mata M, Muñoz MJ, Alló M, Fededa JP, Schor IE & Kornblihtt AR (2011) RNA Polymerase II Elongation at the Crossroads of Transcription and Alternative Splicing. *Genet. Res. Int.* **2011:** 1–9

Dujardin G, Lafaille C, Petrillo E, Buggiano V, Gómez Acuña LI, Fiszbein A, Godoy Herz MA, Nieto Moreno N, Muñoz MJ, Alló M, Schor IE & Kornblihtt AR (2013) Transcriptional elongation and alternative splicing. *Biochim. Biophys. Acta - Gene Regul. Mech.* **1829:** 134–140

Dujardin G, Lafaille C, de la Mata M, Marasco LE, Muñoz MJ, Le Jossic-Corcos C, Corcos L & Kornblihtt AR (2014) How Slow RNA Polymerase II Elongation Favors Alternative Exon Skipping. *Mol. Cell* **54**: 683–690

519 Diamant G, Amir-Zilberstein L, Yamaguchi Y, Handa H & Dikstein R (2012) DSIF Restricts
520 NF-κB Signaling by Coordinating Elongation with mRNA Processing of Negative
521 Feedback Genes. *Cell Rep.* **2:** 722–731

522 Fitz J, Neumann T & Pavri R (2018) Regulation of RNA polymerase II processivity by Spt5
523 is restricted to a narrow window during elongation. *EMBO J.* **37:** e97965

524 Fong N, Kim H, Zhou Y, Ji X, Qiu J, Saldi T, Diener K, Jones K, Fu XD & Bentley DL
525 (2014) Pre-mRNA splicing is facilitated by an optimal RNA polymerase II elongation
526 rate. *Genes Dev.* **28**: 2663–2676

527 Fong YW & Zhou Q (2001) Stimulatory effect of splicing factors on transcriptional
528 elongation. *Nature* **414**: 929–933

529 Görnemann J, Kotovic KM, Hujer K & Neugebauer KM (2005) Cotranscriptional
530 spliceosome assembly occurs in a stepwise fashion and requires the cap binding
531 complex. *Mol. Cell* **19:** 53–63

532 Görnemann J, Barrandon C, Hujer K, Rutz B, Rigaut G, Kotovic KM, Faux C, Neugebauer
533 KM & Séraphin B (2011) Cotranscriptional spliceosome assembly and splicing are
534 independent of the Prp40p WW domain. *RNA* **17**: 2119–2129

535 Grainger RJ & Beggs JD (2005) Prp8 protein: At the heart of the spliceosome. *RNA* **11:** 533–
536 557

537 Harlen KM, Trotta KL, Smith EE, Mosaheb MM, Fuchs SM & Churchman LS (2016)
538 Comprehensive RNA Polymerase II Interactomes Reveal Distinct and Varied Roles for
539 Each Phospho-CTD Residue. *Cell Rep.* **15:** 2147–2158

540 Hartzog GA & Fu J (2013) The Spt4-Spt5 complex: A multi-faceted regulator of
541 transcription elongation. *Biochim. Biophys. Acta - Gene Regul. Mech.* **1829:** 105–115

542 Hirtreiter A, Damsma GE, Cheung ACM, Klose D, Grohmann D, Vojnic E, Martin ACR,
543 Cramer P & Werner F (2010) Spt4/5 stimulates transcription elongation through the
544 RNA polymerase clamp coiled-coil motif. *Nucleic Acids Res.* **38:** 4040–4051

545 Hoskins AA, Friedman LJ, Gallagher SS, Crawford DJ, Anderson EG, Wombacher R,
546 Ramirez N, Cornish VW, Gelles J & Moore MJ (2011) Ordered and dynamic assembly
547 of single spliceosomes. *Science* **331:** 1289–1295

548 Hoskins AA & Moore MJ (2012) The spliceosome: A flexible, reversible macromolecular
549 machine. *Trends Biochem. Sci.* **37:** 179–188

550 Howe KJ, Kane CM & Ares M (2003) Perturbation of transcription elongation influences the
551 fidelity of internal exon inclusion in Saccharomyces cerevisiae. *RNA* **9**: 993–1006

552 Ip JY, Schmidt D, Pan Q, Ramani AK, Fraser AG, Odom DT & Blencowe BJ (2011) Global
553 impact of RNA polymerase II elongation inhibition on alternative splicing regulation.
554 *Genome Res.* **21**: 390–401

555 Jaehning JA (2010) The Paf1 complex: Platform or player in RNA polymerase II
556 transcription? *Biochim. Biophys. Acta - Gene Regul. Mech.* **1799:** 379–388

557 Khodor YL, Menet JS, Tolan M & Rosbash M (2012) Cotranscriptional splicing efficiency
558 differs dramatically between Drosophila and mouse. *RNA* **18:** 2174–2186

559 Klein BJ, Bose D, Baker KJ, Yusoff ZM, Zhang X & Murakami KS (2011) RNA polymerase
560 and transcription elongation factor Spt4/5 complex structure. *Proc. Natl. Acad. Sci.* **108:**
561 546–550

562 Kotovic KM, Lockshon D, Boric L & Neugebauer KM (2003) Cotranscriptional Recruitment
563 of the U1 snRNP to Intron-Containing Genes in Yeast. *Mol. Cell. Biol.* **23:** 5768–5779

564 Kornblihtt AR, De La Mata M, Fededa JP, Muñoz MJ & Nogués G (2004) Multiple links
565 between transcription and splicing. *RNA* **10:** 1489–1498

566 Krogan NJ, Dover J, Wood A, Schneider J, Heidt J, Boateng MA, Dean K, Ryan OW,
567 Golshani A, Johnston M, Greenblatt JF & Shilatifard A (2003) The Paf1 complex is
568 required for histone H3 methylation by COMPASS and Dot1p: Linking transcriptional
569 elongation to histone methylation. *Mol. Cell* **11:** 721–729

570 Lacadie SA & Rosbash M (2005) Cotranscriptional spliceosome assembly dynamics and the
571 role of U1 snRNA:5′ss base pairing in yeast. *Mol. Cell* **19:** 65–75

572 Laribee RN, Krogan NJ, Xiao T, Shibata Y, Hughes TR, Greenblatt JF & Strahl BD (2005)
573 BUR kinase selectively regulates H3 K4 trimethylation and H2B ubiquitylation through
574 recruitment of the PAF elongation complex. *Curr. Biol.* **15:** 1487–1493

575 Li Y, Xia C, Feng J, Yang D, Wu F, Cao Y, Li L & Ma L (2016) The SNW Domain of SKIP
576 Is Required for Its Integration into the Spliceosome and Its Interaction with the Paf1
577 Complex in Arabidopsis. *Mol. Plant* **9:** 1040–1050

578 Lindstrom DL, Squazzo SL, Muster N, Burckin TA, Wachter KC, Emigh CA, McCleery JA,
579 Yates JR & Hartzog GA (2003) Dual Roles for Spt5 in Pre-mRNA Processing and
580 Transcription Elongation Revealed by Identification of Spt5-Associated Proteins. *Mol.*
581 *Cell. Biol.* **23:** 1368–1378

582 Listerman I, Sapra AK & Neugebauer KM (2006) Cotranscriptional coupling of splicing
583 factor recruitment and precursor messenger RNA splicing in mammalian cells. *Nat.*
584 *Struct. Mol. Biol.* **13:** 815–822

585 Liu CR, Chang CR, Chern Y, Wang TH, Hsieh WC, Shen WC, Chang CY, Chu IC, Deng N,
586 Cohen SN & Cheng TH (2012) Spt4 is selectively required for transcription of extended
587 trinucleotide repeats. *Cell* **148:** 690–701

588 Liu Y, Warfield L, Zhang C, Luo J, Allen J, Lang WH, Ranish J, Shokat KM & Hahn S
589 (2009) Phosphorylation of the Transcription Elongation Factor Spt5 by Yeast Bur1
590 Kinase Stimulates Recruitment of the PAF Complex. *Mol. Cell. Biol.* **29:** 4852–4863

591 Martinez-Rucobo FW, Sainsbury S, Cheung ACM & Cramer P (2011) Architecture of the
592 RNA polymerase-Spt4/5 complex and basis of universal transcription processivity.
593 *EMBO J.* **30:** 1302–1310

594 McIsaac RS, Gibney PA, Chandran SS, Benjamin KR & Botstein D (2014) Synthetic biology
595 tools for programming gene expression without nutritional perturbations in
596 Saccharomyces cerevisiae. *Nucleic Acids Res.* **42:** e48

597 Mendoza-Ochoa GI, Barrass JD, Terlouw BR, Maudlin IE, de Lucas S, Sani E, Aslanzadeh
598 V, Reid JAE & Beggs JD (2018) A fast and tuneable auxin-inducible degron for
599 depletion of target proteins in budding yeast. *Yeast*

600 Merkhofer EC, Hu P & Johnson TL (2014) Introduction to cotranscriptional RNA splicing.
601 *Methods Mol. Biol.* **1126:** 83–96

602 Mili S & Steitz JA (2004) Evidence for reassociation of RNA-binding proteins after cell
603 lysis: Implications for the interpretation of immunoprecipitation analyses. *RNA* **10**:
604 1692–1694

605 Moore MJ, Schwartzfarb EM, Silver PAA & Yu MC (2006) Differential Recruitment of the
606 Splicing Machinery during Transcription Predicts Genome-Wide Patterns of mRNA
607 Splicing. *Mol. Cell* **24:** 903–915

608 Morawska M & Ulrich HD (2013) An expanded tool kit for the auxin-inducible degron
609 system in budding yeast. *Yeast* **30:** 341–351

610 Neugebauer KM (2002) On the importance of being co-transcriptional. *J. Cell Sci.* **115:**
611 3865–3871

612 Ng HH, Dole S & Struhl K (2003) The Rtf1 Component of the Paf1 Transcriptional
613 Elongation Complex Is Required for Ubiquitination of Histone H2B. *J. Biol. Chem.* **278:**
614 33625–33628

615 Nishimura K, Fukagawa T, Takisawa H, Kakimoto T & Kanemaki M (2009) An auxin-based
616 degron system for the rapid depletion of proteins in nonplant cells. *Nat. Methods* **6:**
617 917–922

618 Nojima T, Gomes T, Grosso ARF, Kimura H, Dye MJ, Dhir S, Carmo-Fonseca M &
619 Proudfoot NJ (2015) Mammalian NET-seq reveals genome-wide nascent transcription
620 coupled to RNA processing. *Cell* **161:** 526–540

621 Perales R & Bentley D (2009) 'Cotranscriptionality': The Transcription Elongation Complex
622 as a Nexus for Nuclear Transactions. *Mol. Cell* **36:** 178–191

623 Shetty A, Kallgren SP, Demel C, Maier KC, Spatt D, Alver BH, Cramer P, Park PJ &
624 Winston F (2017) Spt5 Plays Vital Roles in the Control of Sense and Antisense
625 Transcription Elongation. *Mol. Cell* **66:** 77–88.e5

626 Tardiff DF & Rosbash M (2006) Arrested yeast splicing complexes indicate stepwise snRNP
627 recruitment during in vivo spliceosome assembly. *Rna* **12:** 968–979

628 Tilgner H, Knowles DG, Johnson R, Davis CA, Chakrabortty S, Djebali S, Curado J, Snyder
629 M, Gingeras TR & Guigó R (2012) Deep sequencing of subcellular RNA fractions
630 shows splicing to be predominantly co-transcriptional in the human genome but
631 inefficient for lncRNAs. *Genome Res.* **22:** 1616–1625

632 Tseng CK & Cheng SC (2008) Both catalytic steps of nuclear pre-mRNA splicing are
633 reversible. *Science* **320:** 1782–1784

634 Volland C, Urban-Grimal D, Géraud G & Haguenauer-Tsapis R (1994) Endocytosis and
635 degradation of the yeast uracil permease under adverse conditions. *J. Biol. Chem.* **269:**
636 9833–9841

637 Wallace EWJ & Beggs JD (2017) Extremely fast and incredibly close: Cotranscriptional
638 splicing in budding yeast. *RNA* **23:** 601–610

639 Wiesner S, Stier G, Sattler M & Macias MJ (2002) Solution structure and ligand recognition
640 of the WW domain pair of the yeast splicing factor Prp40. *J. Mol. Biol.* **324:** 807–822

641 Will CL & Lührmann R (2011) Spliceosome structure and function. *Cold Spring Harb.*
642 *Perspect. Biol.* **3:** 1–2

643 Wood A, Schneider J, Dover J, Johnston M & Shilatifard A (2003) The Paf1 complex is
644 essential for histone monoubiquitination by the Rad6-Bre1 complex, which signals for
645 histone methylation by COMPASS and Dot1p. *J. Biol. Chem.* **278:** 34739–34742

646 Xiao Y, Yang YH, Burckin TA, Shiue L, Hartzog GA & Segal MR (2005a) Analysis of a
647 splice array experiment elucidates roles of chromatin elongation factor Spt4-5 in
648 splicing. *PLoS Comput. Biol.* **1:** 0276–0288

649 Xiao T, Kao C-F, Krogan NJ, Sun Z-W, Greenblatt JF, Osley MA & Strahl BD (2005b)
650 Histone H2B Ubiquitylation Is Associated with Elongating RNA Polymerase II. *Mol.*
651 *Cell. Biol.* **25:** 637–651

652 Zhou K, Kuo WHW, Fillingham J & Greenblatt JF (2009) Control of transcriptional
653 elongation and cotranscriptional histone modification by the yeast BUR kinase substrate
654 Spt5. *Proc. Natl. Acad. Sci.* **106:** 6956–6961

655
656

Figure legends

Figure 1. Use of the AID system to conditionally deplete Spt5.

(A) Western blot probed with anti-FLAG and anti-Pgk1 as a loading control. Samples were taken before (T0) and 40 minutes (T40) after addition of auxin and β-estradiol. Spt5-AID* depletion was quantified and shown as the percentage mean of 3 biological replicates for T40 relative to T0 and normalised to the Pgk1 signal. Error bars = standard error of the mean. Gray crosses indicate the individual replicate values.

(B) A diagram drawn to scale, showing the positions of amplicons used for ChIP-qPCR analyses across each of the intron-containing genes *ACT1*, *RPS13*, *ECM33*. Exons are represented by gray rectangles and a scale bar of 1 kb is shown.

(C) Anti-FLAG ChIP followed by qPCR analysis of the intron-containing genes *ACT1*, *RPS13*, *ECM33* without (-) auxin and β-estradiol (solid black line) or (+) 40 minutes after auxin and β-estradiol (dashed black line) addition to deplete Spt5-AID*-6FLAG. The X-axis of each graph shows the amplicons used for ChIP qPCR analysis. The data are presented as the mean percentage of input relative to the first amplicon of each gene for at least three biological replicates. Error bars = standard error of the mean. Asterisks show the statistical significance (Student's unpaired t-test). *P < 0.05, ** P <0.01 and *** P < 0.001. Not significant = P > 0.05. Gray crosses indicate the individual replicate values without auxin and β-estradiol and gray circles indicate the individual replicate values 40 minutes after auxin and β-estradiol addition.

Figure 2. Depletion of Spt5 reduces co-transcriptional recruitment of U5 snRNPs

(A) Anti-Prp40 (U1 snRNP), (B) anti-Lea1-HA (U2 snRNP), (C) anti-Prp8 (U5 snRNP) and (D) anti-Rpb1 (RNAPII) ChIP and qPCR across intron-containing genes *ACT1*, *RPS13* and

682 *ECM33* without auxin or β-estradiol (solid black line) and with 40 minutes of auxin and β-
683 estradiol treatment to deplete Spt5-AID* (dashed black line). The X-axes show the amplicons
684 used for ChIP qPCR analysis (see Figure 1B). The ChIP data are presented as the mean
685 percentage of input relative to the first amplicon of each gene for at least 3 biological replicates.
686 Error bars = standard error of the mean. Gray crosses indicate the individual replicate values
687 without auxin and β-estradiol and gray circles indicate the individual replicate values 40
688 minutes after auxin and β-estradiol addition. (E) Western blot probed with anti-Prp8 (U5
689 snRNP), anti-FLAG and anti-PGK1 as a loading control. T0, samples taken before, and T40,
690 40 minutes after addition of auxin and β-estradiol. Quantification of Prp8 is presented as the
691 percentage mean of 3 biological replicates for T40 samples relative to T0 values and
692 normalised to the PGK1 signal. Error bars = standard error of the mean. Asterisks show the
693 statistical significance (Student's unpaired t-test). *P < 0.05, ** P <0.01 and *** P < 0.001.
694 Not significant = P > 0.05. Gray crosses indicate the individual replicate values.

695 **Figure 3. Depletion of Spt5 affects pre-mRNA splicing.**

696 (A) Cartoon showing the RT-qPCR amplicons for splicing analysis for an average gene. These
697 detect pre-mRNA (5'SS or BP and 3'SS), lariat (excised intron or intron-exon 2), exon 2 (ex
698 2) and mRNA.
699 (B) RT-qPCR analysis of the intron-containing genes *ACT1*, *RPS13* and *ECM33* after depletion
700 of Spt5-AID*, normalised to the *SCR1* RNAPIII transcript and time zero (without auxin and
701 β-estradiol addition). Mean of 3 biological replicates. Error bars = standard error of the mean.
702 Asterisks show the statistical significance (Student's unpaired t-test). *P < 0.05, ** P <0.01
703 and *** P < 0.001. Not significant = P > 0.05. Gray crosses indicate the individual replicate
704 values.
705
706

Figure 4. Spt5 interacts with snRNPs.

(A) RIP experiment in which Spt5-AID*-6FLAG was pulled down followed by RT-qPCR using primers against snRNAs U1, U2, U4, U5 and U6 (white bars). A mock pulldown was also performed (gray bars). Data are normalised to the input. Error bars = standard deviation of 3 biological replicates.

(B) RIP experiment in which Spt5-AID*-6FLAG was pulled down followed by RT-qPCR using primers for the intron-containing genes *ACT1*, *RPS13* and *ECM33* (white bars). A mock pulldown was also performed (gray bars). Data are normalised as percentage of input (% input). Error bars = standard deviation of 3 biological replicates.

(C) Western blots from a co-immunoprecipitation experiment in which Spt5-AID*-6FLAG was pulled down using anti-FLAG antibody with or without RNase treatment, blotted and probed with anti-Prp40 (U1 snRNP), anti-Lea-3HA (U2 snRNP) and anti-Prp8 (U5 snRNP) antibodies, then probed with anti-FLAG antibody. Additionally, an untagged Spt5 control strain with Lea1-3HA tagged was used for a pull-down with the FLAG antibody as a negative control. Input (10%), non-bound (NB) and immunoprecipitation (IP) samples were loaded.

(D) Western blots from co-immunoprecipitation experiments in which the U1 snRNP, U2 snRNP or U5 snRNP were pulled down using anti-Prp40, anti-HA (for Lea1-HA) or anti-Prp8 respectively in the Spt5-AID*-6FLAG strain with Lea1-3HA tagged. Additionally, a negative rabbit IgG control was included in which rabbit IgG was used for a pull-down with the Spt5-AID*-6FLAG strain with Lea1-3HA tagged. Input (10%), non-bound and immunoprecipitation (IP) samples were loaded. The blot was probed with antibodies against Prp8 (U5 snRNP), FLAG (Spt5-AID*-6FLAG), Prp40 (U1 snRNP) and HA (Lea1-3HA) (U2 snRNP).

(E) RT-qPCR analysis to determine efficiency of RNase treatment of samples used for co-immunoprecipitation in Figures 4C and 4D. Primers were used against snRNAs U1, U2, U4,

U5 and U6 and *ACT1* (mRNA, 3'SS, BP, Lariat and Exon 2). Data are shown as % RNA remaining relative to conditions without RNase treatment. Mean of 2 biological replicates. Error bars = standard deviation.

Figure 5. Paf1 depletion does not affect recruitment of U5 snRNP or pre-mRNA splicing.

(A) Western blot probed with anti-FLAG and anti-Pgk1 as a loading control. T0, samples taken before or T30, 30 minutes after addition of auxin. Paf1-AID* depletion was quantified and shown as the percentage mean of 3 biological replicates of T30 relative to T0 values and normalised to the Pgk1 signal. Error bars = standard error of the mean. Gray crosses indicate the individual replicate values.

(B) Anti-FLAG (Paf1-AID*) and (C) anti-Prp8 (U5 snRNP) ChIP followed by qPCR analysis of the intron-containing genes: *ACT1*, *RPS13*, *ECM33,* 0 minutes (no auxin; solid black line) and 30 minutes (+ auxin; dashed black line) after auxin addition to deplete Paf1-AID*. X-axes show amplicons used for ChIP qPCR analysis (see Figure 1B). Data are presented as mean percentage of input relative to the first amplicon of each gene. Mean of at least three biological replicates. Error bars = standard error of the mean. Asterisks show the statistical significance (Student's unpaired t-test). *P < 0.05, ** P <0.01 and *** P < 0.001. Not significant = P > 0.05. Gray crosses indicate the individual replicate values without auxin and β-estradiol and gray circles indicate the individual replicate values 40 minutes after auxin and β-estradiol addition.

(D) RT-qPCR analysis of total RNA from the intron-containing genes *ACT1*, *RPS13* and *ECM33* after 30 minutes of depletion of Paf1-AID* (A). Normalised to the *SCR1* RNAPIII transcript and time zero (no auxin). Primers used detected pre-mRNA (5'SS or BP and 3'SS), lariat (excised intron or intron-exon 2), exon 2 (ex 2) and mRNA (see figure 3.6A for cartoon).

Mean of 3 biological replicates. Error bars = standard error of the mean. Gray crosses indicate the individual replicate values.

Figure 6. Model: a role for Spt5 in co-transcriptional spliceosome assembly.

In wild-type (WT) conditions (without Spt5 depletion), Spt5 facilitates co-transcriptional spliceosome assembly by promoting stable recruitment of the U5 snRNP. This may be mediated, either directly or indirectly, by interaction between Spt5 and core members of the spliceosome although it is unclear whether the interaction occurs already at the pre-spliceosome stage. Upon Spt5 depletion (indicated by the red cross), the U5 snRNP is either not recruited or does not remain stably associated, so that pre-B/B complexes or later complexes do not form, or form and then rapidly disassemble, leading to defects in splicing catalysis.

Supplementary Figure S1.

RT-qPCR analysis of the intron-containing transcripts of *ACT1* (A), *RPS13* (B) and *ECM33* (C) before (T0) and after (T40) depletion of Spt5-AID*, normalised to the *SCR1* RNAPIII transcript. Mean of 3 biological replicates. Error bars = standard error of the mean. Gray crosses indicate the individual replicate values. Due to different efficiencies of PCR probes, the levels of different RNA species cannot be closely compared.

Supplementary Figure S2.

RT-qPCR analysis of the intron-containing transcripts of *ACT1* (A), *RPS13* (B) and *ECM33* (C) before (T0) and after (T30) depletion of Paf1-AID*, normalised to the *SCR1* RNAPIII transcript. Mean of 3 biological replicates. Error bars = standard error of the mean. Gray crosses indicate the individual replicate values. Due to different efficiencies of PCR probes, the levels of different RNA species cannot be closely compared.

781 **Table 1. Yeast strains used in this study**

Name	Genotype	Source
W303	*MATα ade2-1 ura3-1 his3-11,15 trp1-1 leu2-3,112 can1-100*	Beggs lab
W303 (PADH1-409-TIR1)	*MATα ade2-1 ura3-1 trp1-1 leu2-3,112 can1-100 his3-11,15::PADH1-397-OsTIR1*	Mendoza-Ochoa et al. 2018
W303 (PADH1-409-TIR1) Paf1-AID*-6FLAG Lea1-3HA	*MATα ade2-1 ura3-1 trp1-1 leu2-3,112 can1-100 his3-11,15::PADH1-397-OsTIR1 PAF1-AID*-6FLAG-HygMX LEA1-3HA-KAN*	This study
W303 Spt5-AID*-6FLAG Lea1-3HA pBest-TIR1-LEU2	*MATα ade2-1 ura3-1 trp1-1 leu2-3,112 can1-100 his3-11,15 SPT5-AID*-6FLAG-HygMX LEA1-3HA-KAN* [pBest-*TIR1-LEU2]*	This study
W303 Lea1-3HA	*MATα ade2-1 ura3-1 trp1-1 leu2-3,112 can1-100 his3-11,15 LEA1-3HA-KAN*	This study

782

783 **Table 2. Antibodies used in this study for western blotting, ChIP, RIP and co-**

784 **imunoprecipitation**

Antibody	Application
Rabbit anti-Prp40 (rabbit 11 Eurogentec 2014)	western blotting
Rabbit anti-Prp8 (R1703 Final bleed Boon peptide 5/046)	western blotting
Rat anti-FLAG (Agilent #200474)	western blotting
Mouse anti-Rpb1 (Diagenode #C15100055-100)	western blotting
Mouse anti-Pgk1 (Abcam #22C5D8)	western blotting
Mouse anti-HA (Santa Cruz #F-7)	western blotting
Goat anti-mouse IRDye680RD (LI-COR #926-68070)	western blotting
Goat anti-rabbit IRDye680RD (LI-COR #926-32223)	western blotting
Goat anti-rat IRDye800RD (LI-COR #926-32219)	western blotting
Goat anti-rabbit IRDye800RD (LI-COR #925-32211)	western blotting
Rabbit anti-Prp40 (rabbit 11 Eurogentec 2014)	ChIP, western blotting
Rabbit anti-Prp8 (R1703 Final bleed Boon peptide 5/046)	ChIP, Co-immunoprecipitation, western blotting
Rabbit anti-HA (Abcam #AB9110)	ChIP, Co-immunoprecipitation
Mouse anti-FLAG (Sigma M2 #F1804)	ChIP, Co-immunoprecipitation, RIP
Mouse anti-Rpb1 (Diagenode #C15100055-100)	ChIP, western blotting

785
786

Figure 1. Use of the AID system to conditionally deplete Spt5

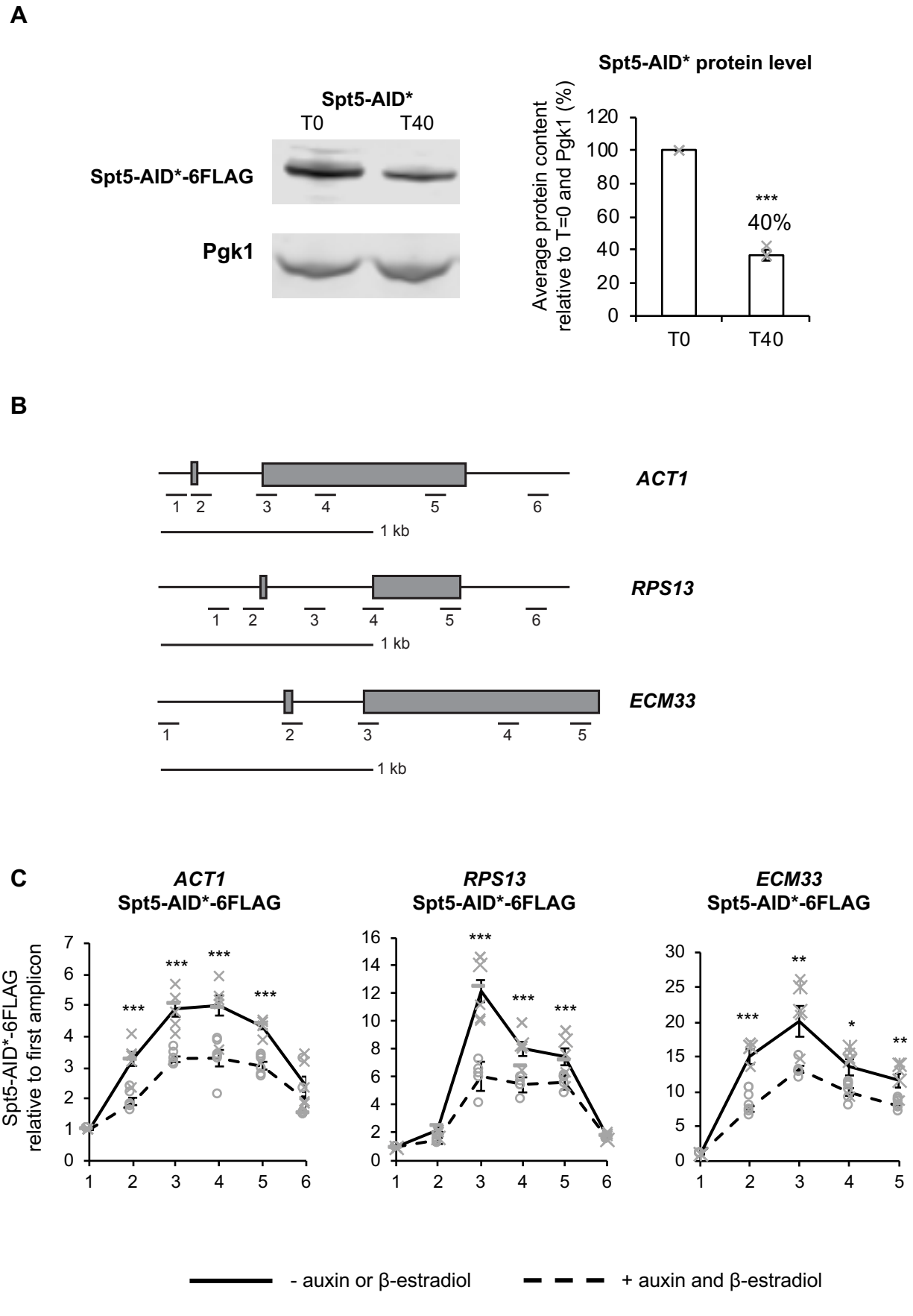

Figure 2. Depletion of Spt5 reduces co-transcriptional recruitment of U5 snRNPs

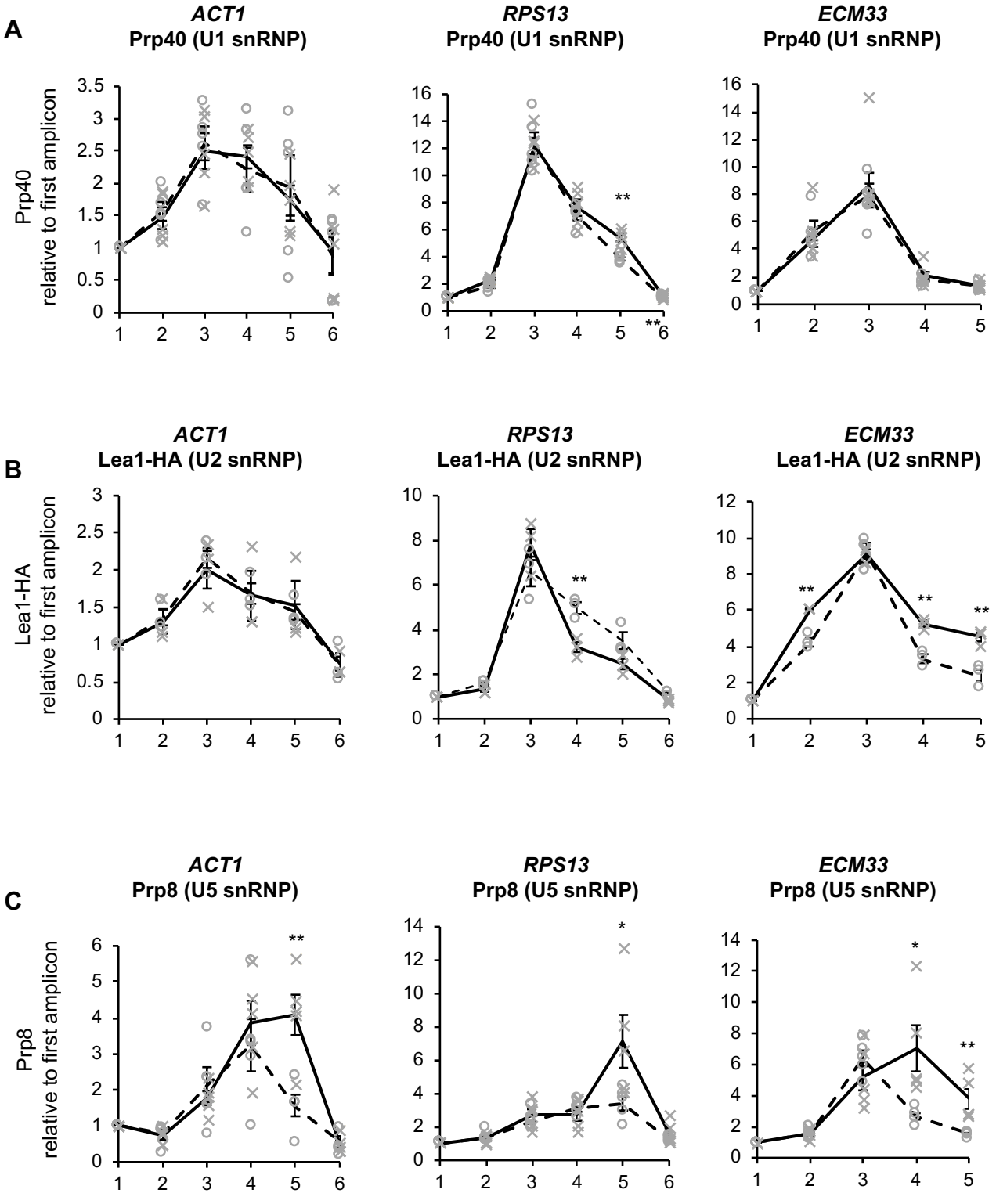

Figure 2. Depletion of Spt5 reduces co-transcriptional recruitment of U5 snRNPs

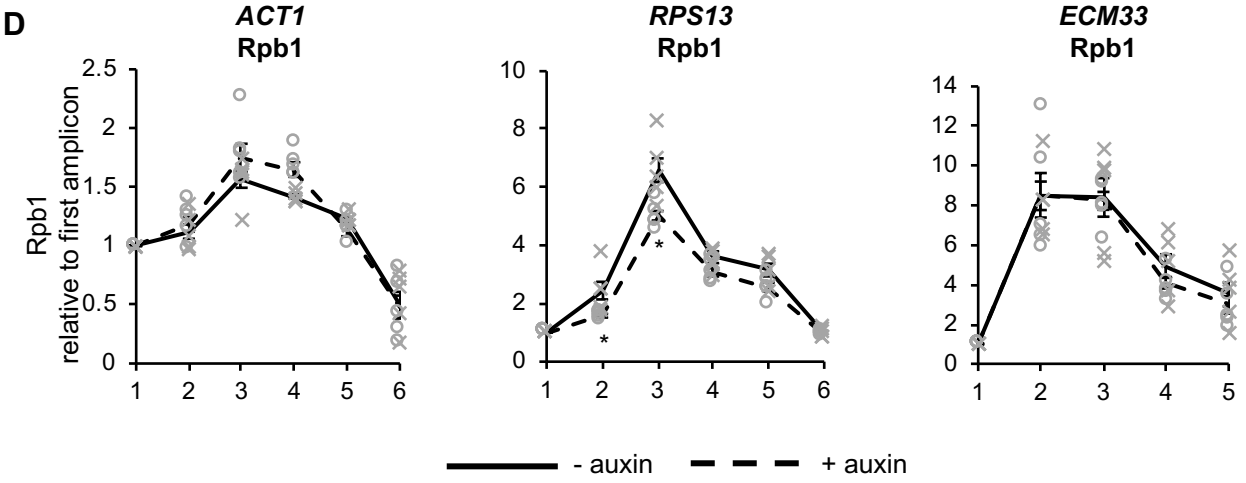

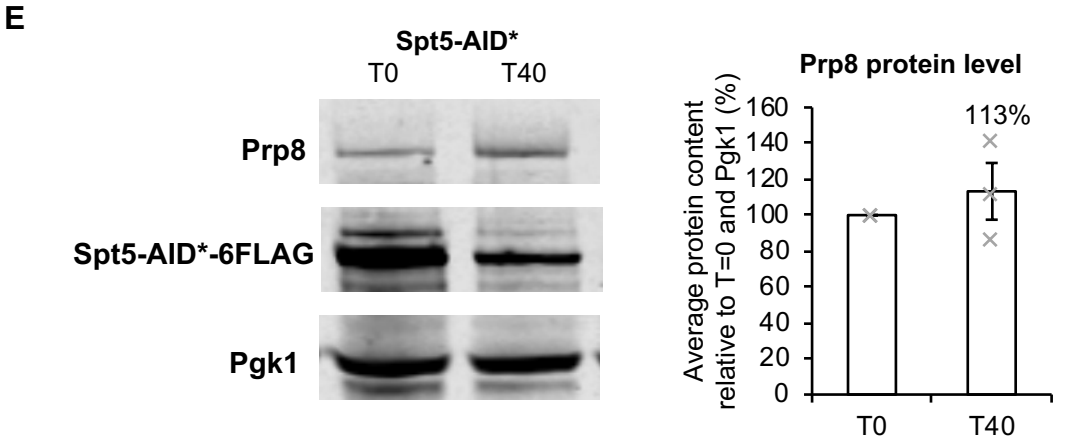

Figure 3. Depletion of Spt5 affects pre-mRNA splicing

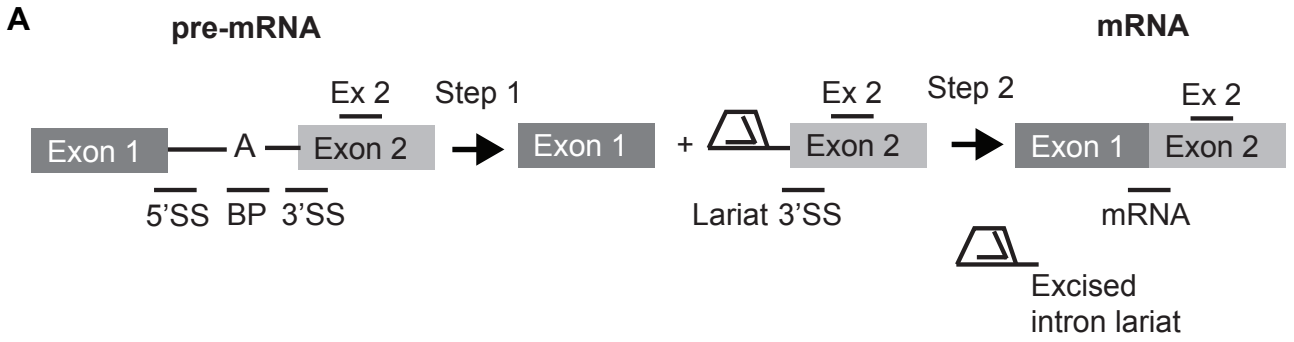

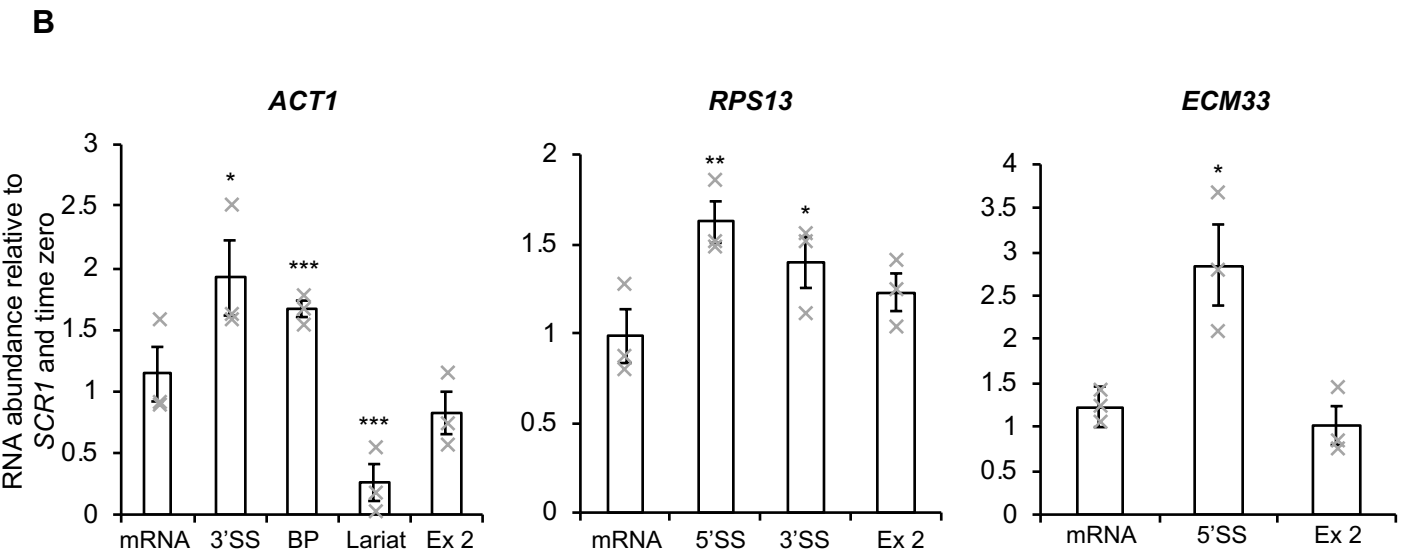

Figure 4. Spt5 interacts with snRNPs

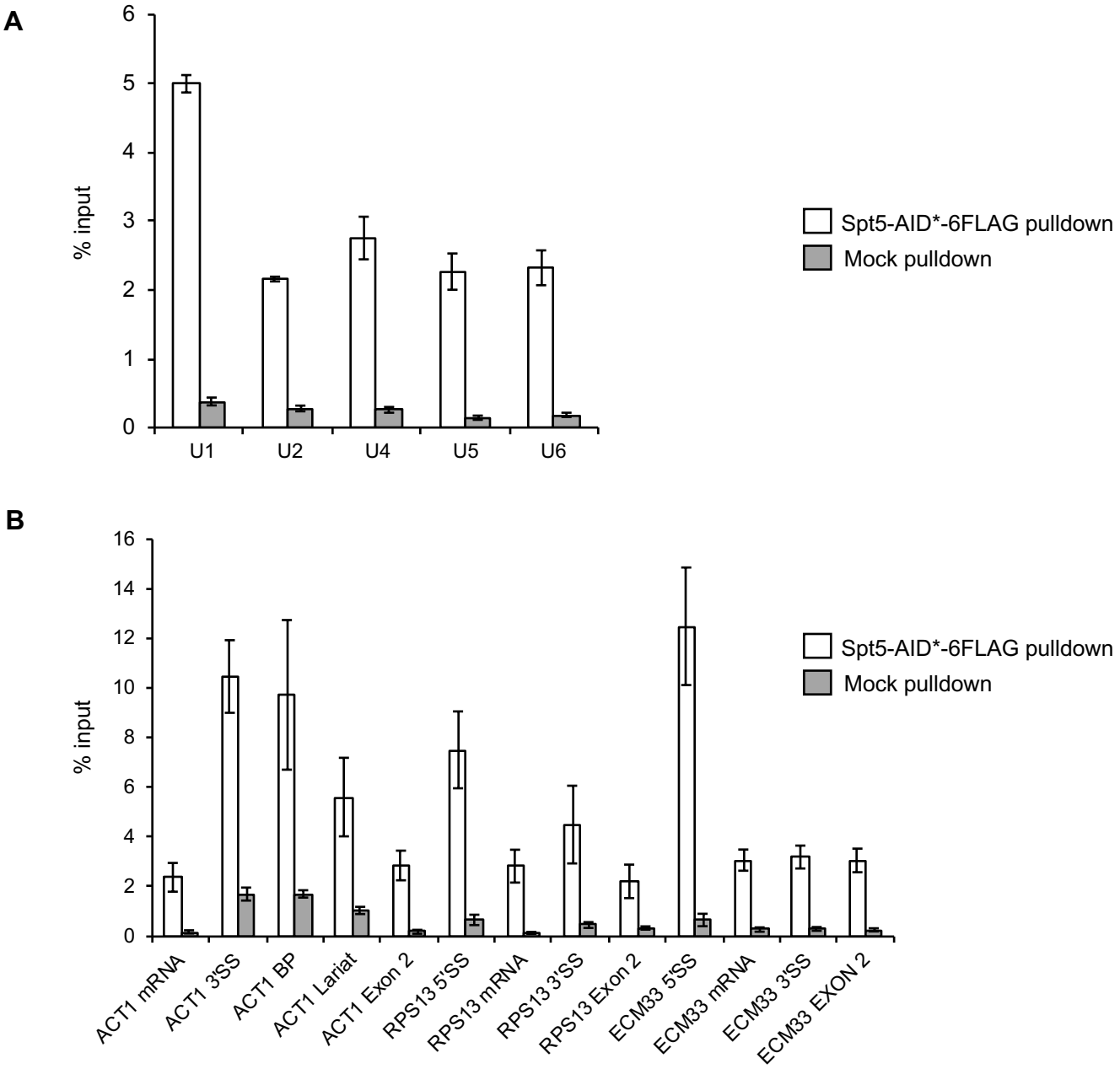

Figure 4. Spt5 interacts with snRNPs

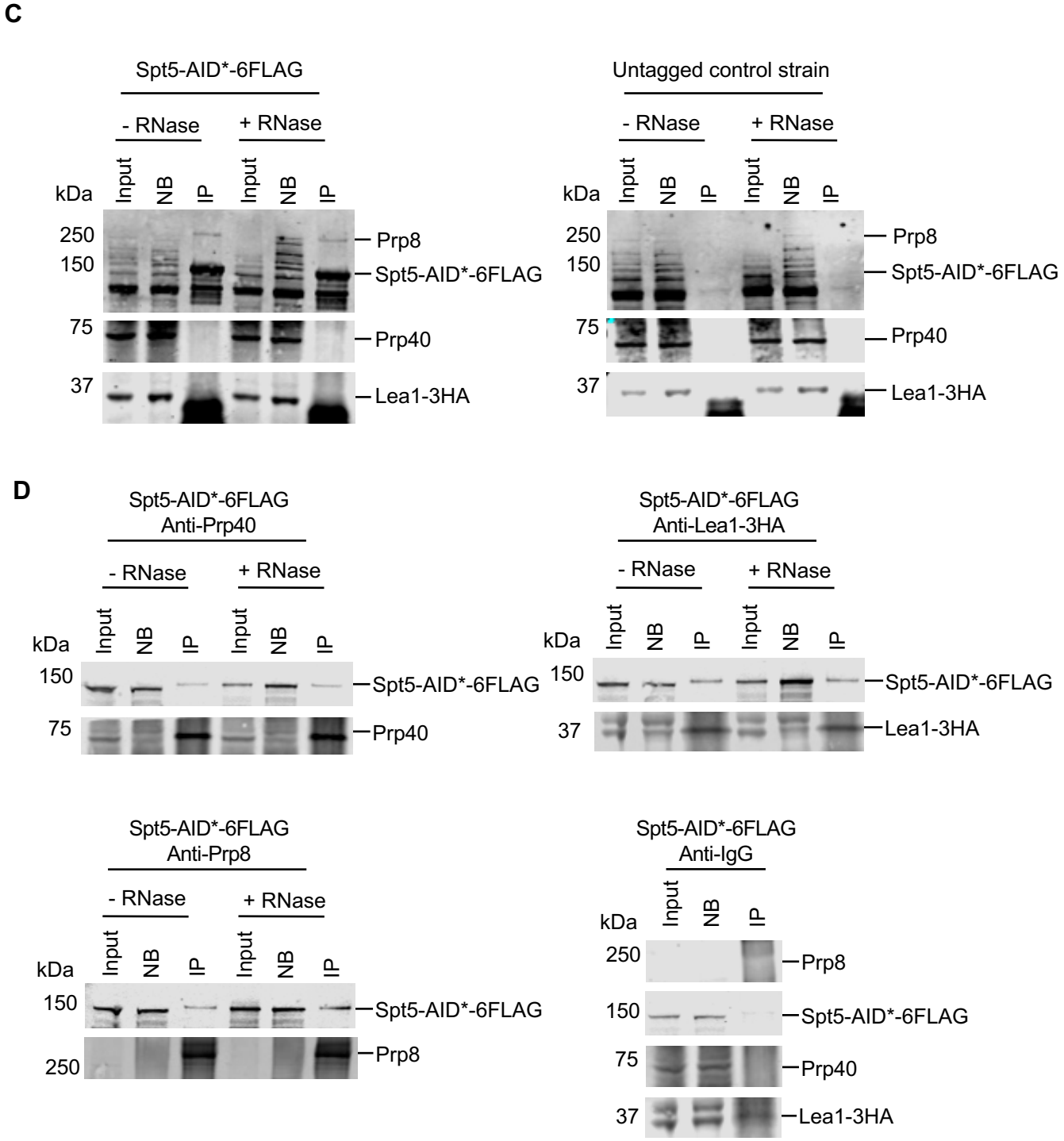

Figure 4. Spt5 interacts with snRNPs

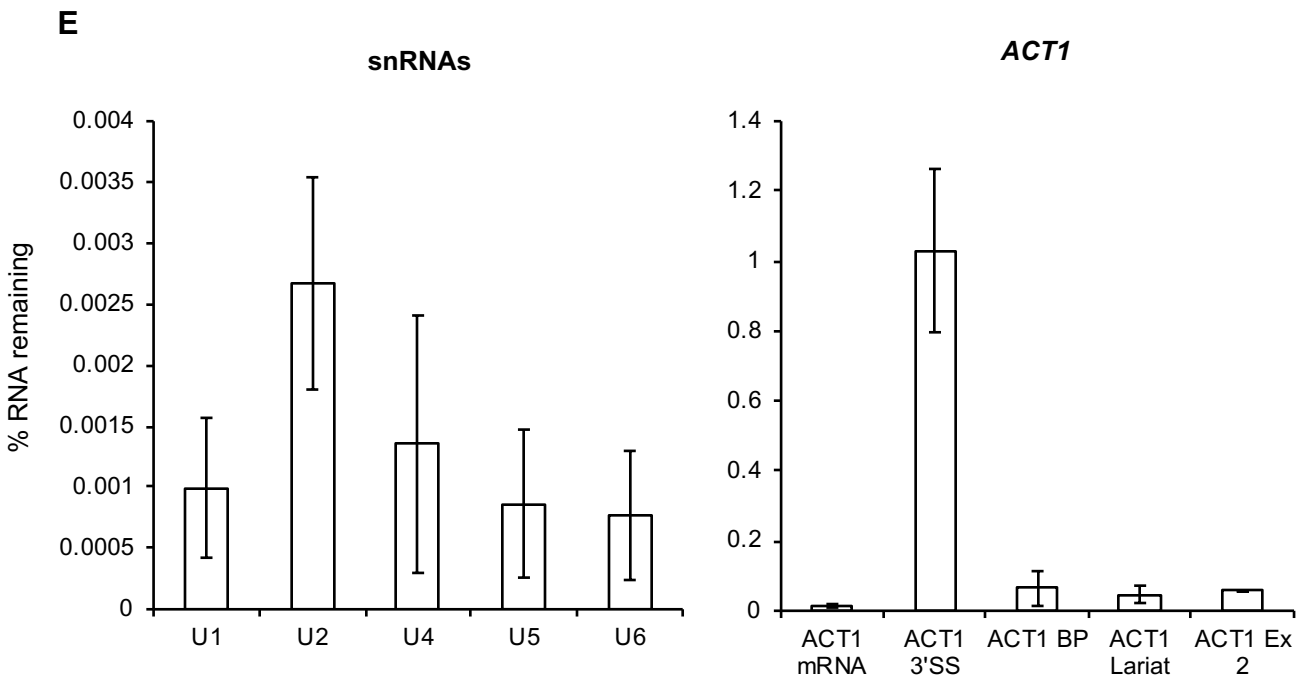

Figure 5. Paf1 depletion does not affect recruitment of U5 snRNP or pre-mRNA splicing

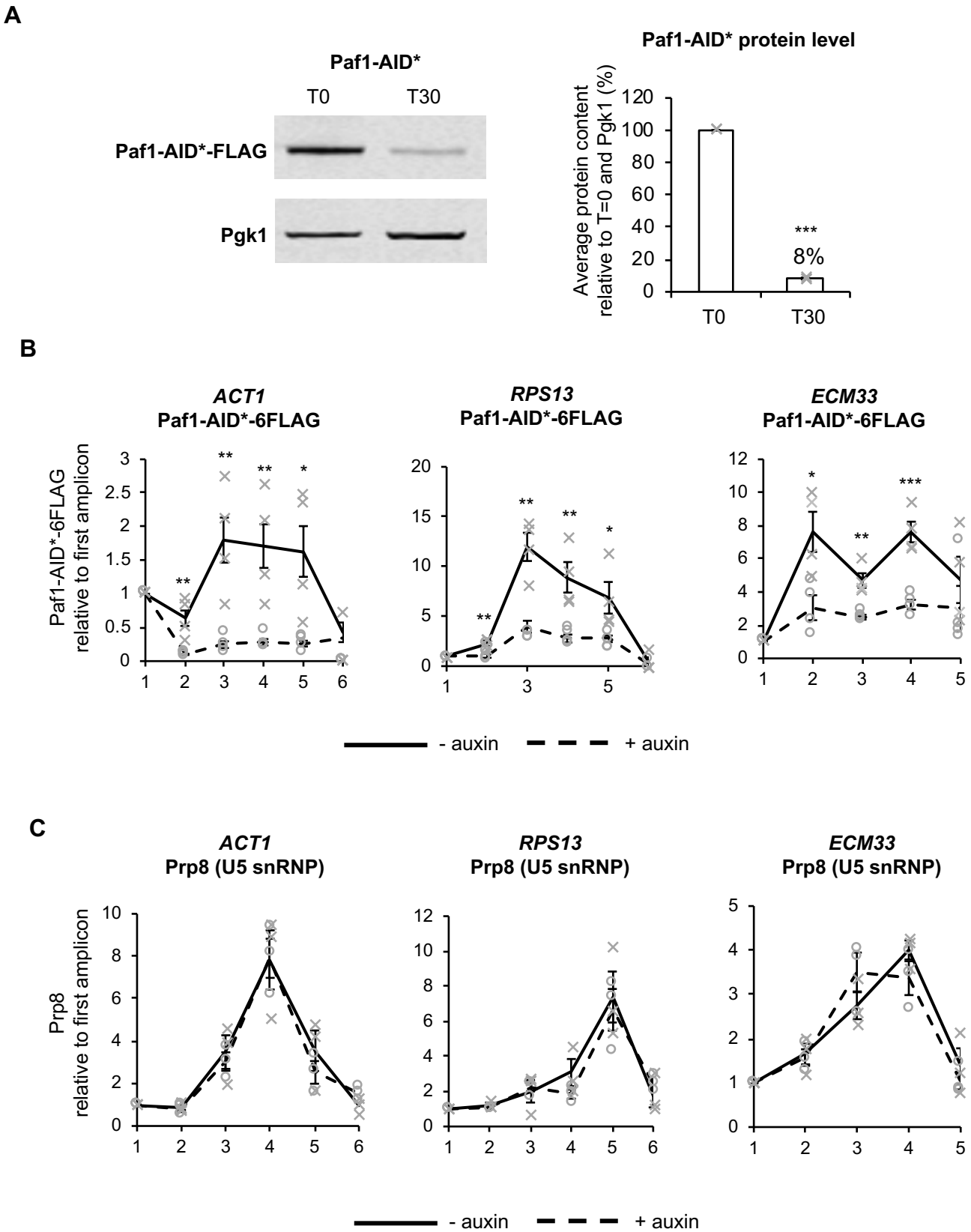

Figure 5. Paf1 depletion does not affect recruitment of U5 snRNP or pre-mRNA splicing

D

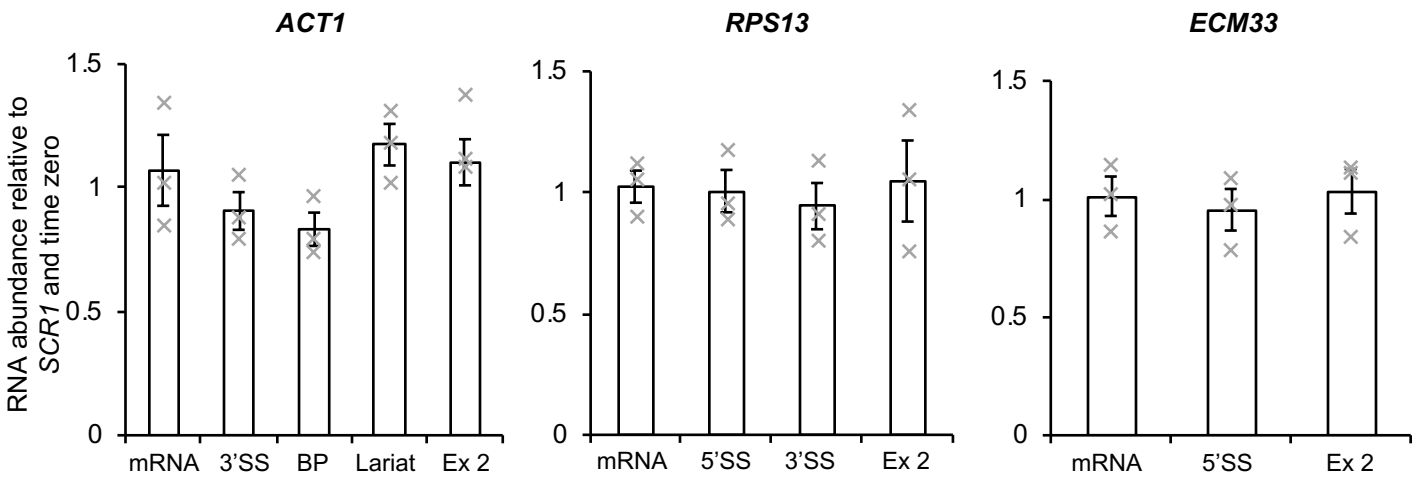

Figure 6. Model: a role for Spt5 in co-transcriptional spliceosome assembly

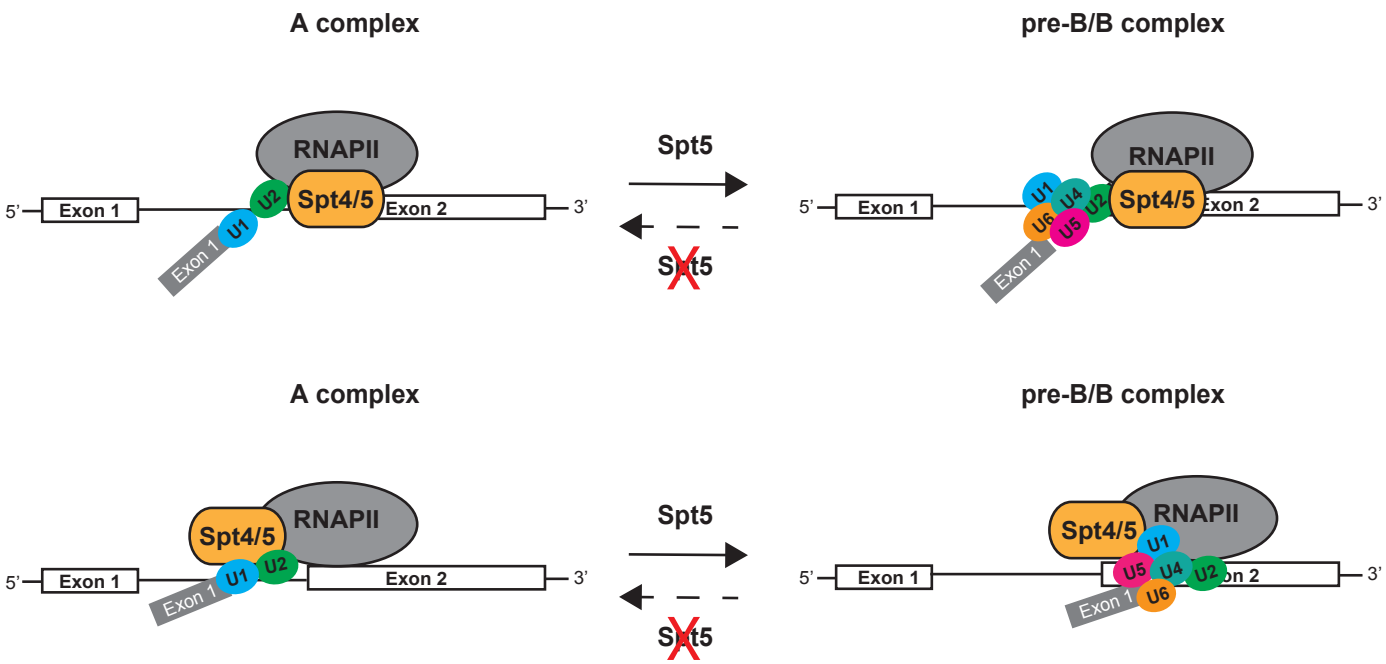

Supplementary Figure S1 (related to Figure 3C)

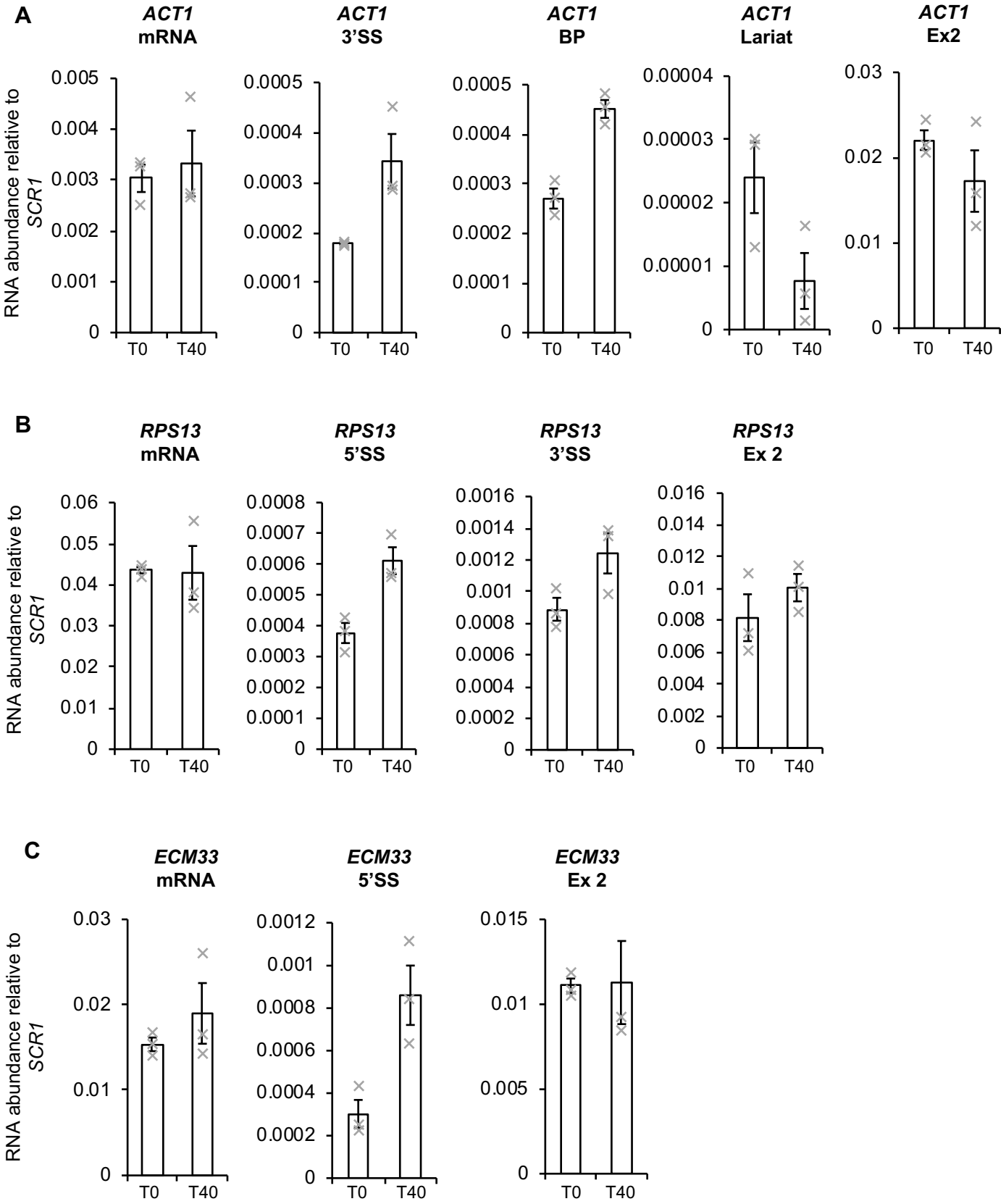

Supplementary Figure S2 (related to Figure 5D)

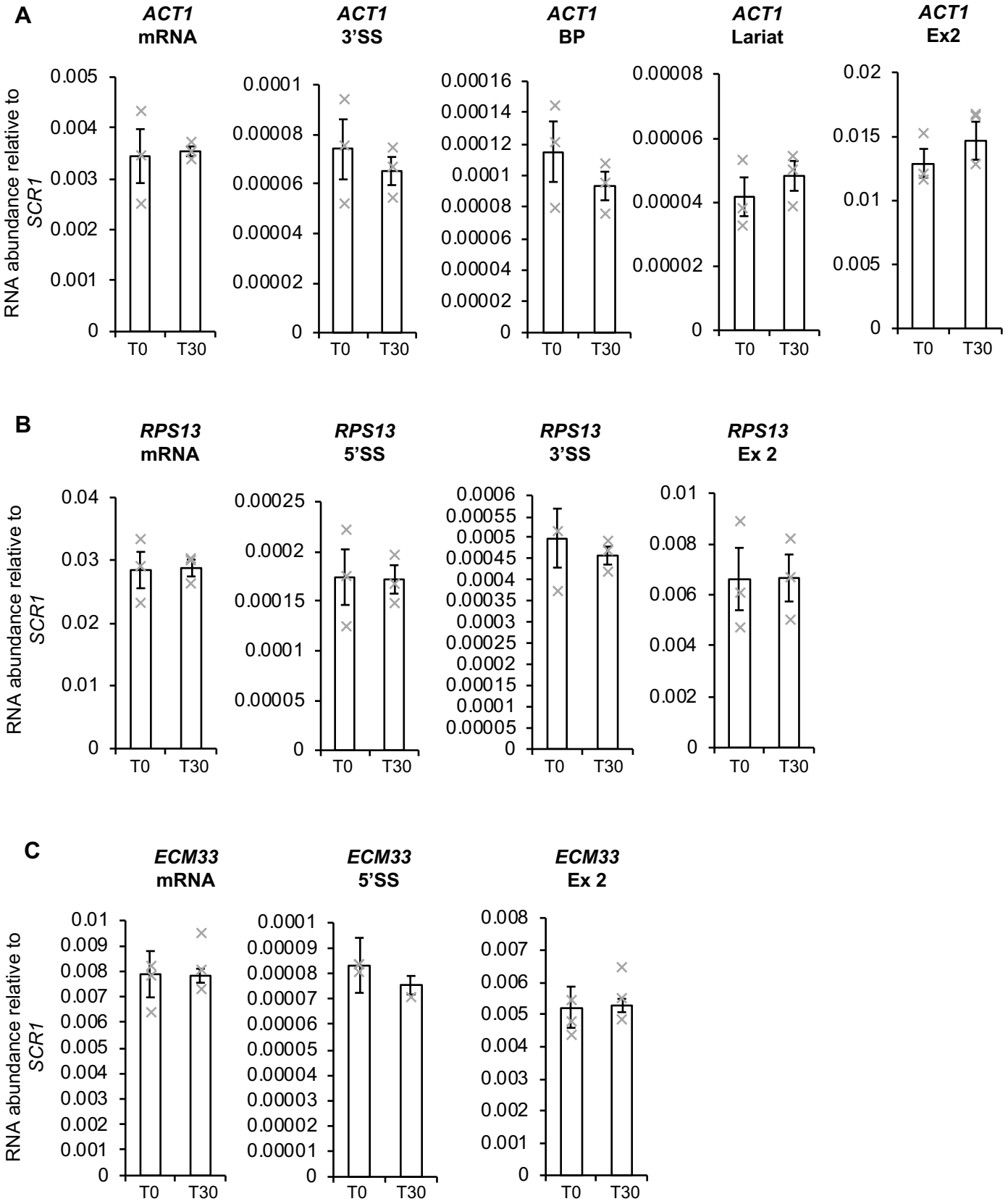

Spt5 modulates co-transcriptional spliceosome assembly in *Saccharomyces cerevisiae*

Isabella E Maudlin and Jean D Beggs

RNA published online July 9, 2019